Optical Percolation and Oxygen Diffusion in Poly(divinylbenzene) Doped Poly(methyl methacrylate) Latex Flms

Ö. Yargı
Department of Physics, Yildiz Technical University, Esenler 34210, Istanbul, Turkey

A simple fluorescence technique is proposed for the measurement of the diffusion coefficient of oxygen into poly(methyl methacrylate) (PMMA) latex-poly(divinylbenzene) (PDVB) composite films. Percolation model was used by using photon transmission (PT) technique to interpret the distribution of PDVB particles in PMMA lattice. Optical results were interpreted according to site percolation theory. The optical percolation threshold value and critical exponent were calculated as, $R_c = 0.03$ and, $\beta = 0.34$, respectively. PT measurements were performed for eight different PDVB content (0, 1.5, 3, 5, 10, 20, 40, and 60) wt%. Pyrene (*P*) functionalized PDVB cross-linked spherical microspheres with diameters of 2.5 μm were synthesized by using precipitation polymerization technique followed by click coupling reaction. The diameter of the PMMA particles prepared by emulsion polymerization was in the range of 0.5–0.7 μm. PMMA/PDVB composite films were then prepared by physically blending of PMMA latex with PDVB microspheres at various compositions. The steady-state fluorescence method was used to monitor oxygen diffusion into these (0, 5, 10, 20, and 40 wt%) latex films. Diffusion coefficients, *D*, of oxygen were determined by the fluorescence quenching method by assuming Fickian transport and were found to be increased from 1.8×10^{-11} to 36.6×10^{-11} $cm^2\ s^{-1}$ with increasing PDVB content. This increase in *D* values was explained with formation of microvoids in the film by using PT technique. POLYM. COMPOS., 34:58–66, 2013. © 2012 Society of Plastics Engineers

INTRODUCTION

Composite materials form a class of materials in which immiscible compounds are combined to obtain new properties [1]. They are heterogeneous mixtures of their components which are generally of quite different properties. Their properties often depart very much from those of the pure components, so that mixing two homogeneous materials into a composite really results in the formation of a new material. Properties depend much more on the morphology and adhesion properties at the interfaces than on the volume fraction of each phase as would happen in an ideal mixture. Because single component polymer films have poor mechanical and gas barrier properties, in last decade, there has been growing interest in producing new materials by filling polymers with inorganic natural (minerals) and/or synthetic (carbon black and silica) compounds[2–6]. These composite materials posses high heat resistance, mechanical strength, and impact resistance or present weak electrical conductivity and low permeability for gases like oxygen or water vapor. These are the major reasons for adding the filler to the matrix. The divinylbenzene (DVB) polymeric materials are widely known and applied as sorbents for gas chromatography [7], as membranes [8, 9], chemical sensors [10], and various coatings [11]. The usual procedure used to measure the diffusion coefficients of gases through polymeric system are based upon measurements of the amount of gas which permeates a given area of polymer in a given time. In addition to this direct method of determination, depending upon the properties of the gases being investigated, there also indirect methods are based on the quenching or bleaching action of these gases on the molecular probes imbedded uniformly in the polymer. Several spectroscopic techniques that use oxygen quenching to determine the rate of oxygen diffusion through polymer films have been reported. The diffusion coefficient of oxygen into poly(methyl methacrylate) (PMMA) was determined by the quenching of phosphorescence of phenanthrene added into polymer [12]. Barker has used the bleaching action of oxygen on color centers produced by electron beam irradiation of polycarbonate and PMMA by following optically the moving boundary [13]. The quenching of fluorescence of naphthalene in PMMA was studied by oxygen in thin films after displacement of nitrogen atmosphere over the sample by oxygen [14]. Cox [15], Cox and Dunn [16], and MacCallum and Rudkin [17] measured oxygen diffusion coefficient by fluorescence quenching in planar sheets of

Correspondence to: Ö. Yargı; e-mail: oyargi@yildiz.edu.tr
DOI 10.1002/pc.22377
Published online in Wiley Online Library (wileyonlinelibrary.com).
© 2012 Society of Plastics Engineers

poly(dimethyl siloxane) [15], filled poly(dimethyl siloxane) sample [16], and polystyrene [17]. They monitored oxygen quenching of a fluorophore as a function of time by assuming that fluorophore dispersed homogeneously within the films. The mathematical determination of D varied, but a single underlying assumption in all cases was that the time-dependent emission intensity measured during the experiment. In some cases, the intensity versus time curve was converted to a concentration versus time curve using the Stern-Volmer relationship [15, 16]. Winnik and Manners [18–20] have used time-scan experiments to measure the decay of luminescence intensity as oxygen diffuses into polymer films under constant illumination and the growth of intensity as oxygen diffuses out of the film. They interpreted their data with the aid of theoretical expressions based on Stern-Volmer quenching kinetics with Fick's laws of diffusion. In some of our earlier studies, we examined the effect of annealing [21] and packing [22] on the oxygen diffusion coefficient, D, in PMMA by using steady-state fluorescence (SSF) and photon transmission (PT) techniques. In these studies, we found that while the D values increased by increasing the film thickness (packing) [22], no temperature effect [21] was observed on the diffusion coefficient, D.

In this study, fluorescence quenching method were used to study oxygen diffusion into PMMA/poly(divinylbenzene) (PDVB) composite films. Transmitted photon intensities, I_{tr} were measured by the UV-visible (UVV) technique to examine latex film morphology. Critical exponent vaule for optical percolation was calculated as, $\beta = 0.34$. A model was developed for low quenching efficiency to measure oxygen diffusion coefficient, D, which change between 1.8×10^{-11} and 36.6×10^{-11} cm^2 s^{-1}. The time drive mode of the SSF spectrometer was used to monitor the intensity change of excited pyrene during oxygen penetration into latex films. The approach was to monitor oxygen quenching of a fluorophore (pyrene), which was believed to be homogeneously dispersed within the films, as a function of time. To determine D values, the quenching is accurately described by a linear Stern-Volmer equation and that the optical density is low enough that the sample is uniformly excited. By fitting the resultant intensity versus time profile to an appropriate diffusion model for the film configuration, an accurate measure of the diffusion coefficients for the composite film were obtained.

EXPERIMENT

Synthesis of PMMA Latex

Unlabeled PMMA latex particles were prepared in a two-step process [23–25]. First, MMA was polymerized to low conversion in cyclohexane in the presence of polyisobutylene (PIB) containing 2% isoprene units to promote grafting. The graft copolymer so produced served as a dispersant in the second stage of polymerization, in which MMA was polymerized in a cyclohexane solution of the polymer. This material, the dispersant, was collected and purified by precipitation with methanol. The dispersant was then added to a second reaction vessel containing cyclohexane, 2,2'-azobis (isobutyronitrile) (AIBN), and MMA. These solutions were refluxed overnight. The reaction became increasingly turbid as it progressed. The latex particles were separated from the solvent and unreacted monomers by repeated cycles of centrifugation, the supernatant liquid was decanted, and the latex particles were redispersed in fresh solvent. These latex dispersions in cyclohexane could be separately freeze-dried and stored as a powder. The produced stable dispersions of spherical polymer latexes range in radius from 0.5 to 0.7 μm (see Fig. 1a). A combination of ^{1}H NMR and UV analysis indicates that these particles contain 4 mol% PIB (These particles were prepared in Professor M.A.Winnik's Laboratory in Toronto.). The molecular weight of graft PMMA was measured as $M_w = 1.10 \times 10^5$ and the polydispersity of the PMMA was 2.3.

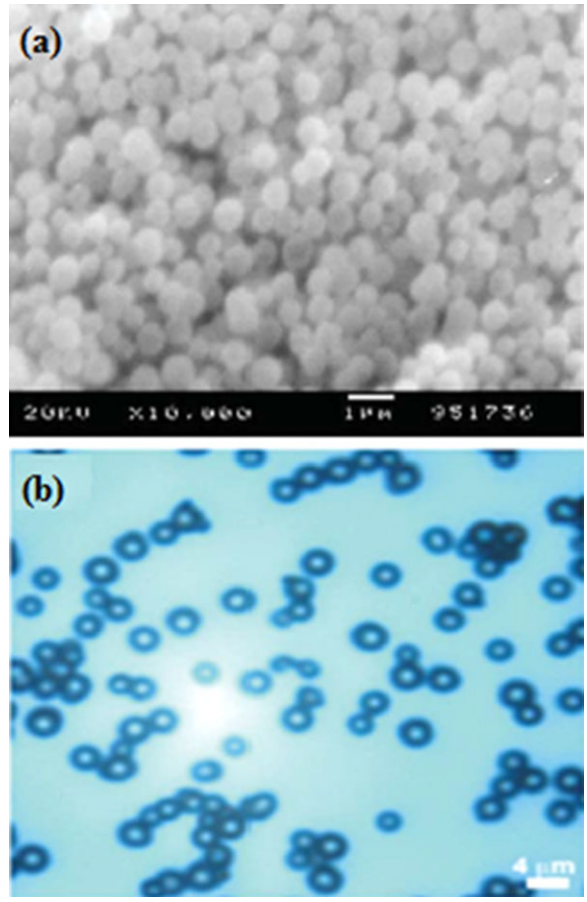


FIG. 1. (a) SEM image of the PMMA particles and (b) optical microscope image of azide functionalized PDVB microspheres. [Color figure can be viewed in the online issue, which is available at wileyonlinelibrary.com.]

Synthesis of Pyrene Functionalized PDVB Microspheres

PDVB microspheres were synthesized via click chemistry strategy [26]. Divinylbenzene (DVB55, 55% mixture of isomers, technical grade, Aldrich) was used as received. Acetonitrile (99%, Aldrich) was distilled over CaH_2 before use. AIBN (Fluka) was recrystallized from methanol. *N,N,N′,N″,N″*-pentamethyldiethylenetriamine (99%, Aldrich) as a ligand was distilled before use. Dichloromethane (CH_2Cl_2, 99% Lab-Scan) was distilled over P_2O_5. *N,N*-Dimethylformamide (99%, Aldrich), sulfuric acid (95–97%, Fluka), potassium bromide (≥ 99.5%, Merck), sodium azide (≥ 99%, Merck), sodium chromate (Merck), silver nitrate (Merck), CuBr (98%, Acros), sodium hydride (98%, Fluka), propargyl bromide (80 vol% in toluene, Fluka), 1-pyrene methanol (98%, Aldrich), methanol (99%, Reiden-de Haön), diethylether (98%, Carlo-Erba), and tetrahydrofuran (THF, 99% Lab-Scan) were used as received.

PDVB microspheres were prepared by precipitation polymerization technique as described in the literature [27]. For this purpose, AIBN (0.2 g, 1.22 mmol, 4 wt% relative to DVB55) was added to the solution of DVB55 (11 mL, 76.8 mmol, 4 vol% relative to total volume) and 274 mL acetonitrile in dry 500 mL volume of three-necked flask equipped with a mechanical stirrer and a nitrogen inlet. The flask was placed in thermostated oil bath and the temperature was adjusted to 70°C. The nitrogen flow was stopped and the reaction was conducted for 48 h at this temperature under continuous stirring (32 rpm). The reaction content was cooled to the room temperature and polymer precipitated was filtered and successively washed with THF (20 mL), acetone (20 mL), and methanol (20 mL). The product was dried at 45°C under vacuum for over night. The yield was 3 g (30%). The residual double bonds on the surface were nearly monodisperse (~2.5 μm) (see Fig. 1b), PDVB microspheres were activated to primary bromine [28, 29] and then converted into azide functions by condensation with NaN_3. Finally, fluorescence labeled PDVB microspheres were obtained by the click reaction [26] with propargyl pyrene [30] through azide functions.

Film Preparation

Composites were prepared by mixing of PMMA latex and pyrene labeled crosslinked PDVB microsphere. For this purpose, PMMA and PDVB particles were dispersed separately in heptane solutions. The dispersion of PDVB in heptane was mixed with the appropriate solutions of PMMA to yield eventually composites with 0, 1.5, 3, 5, 10, 20, 40, and 60 wt% PDVB content. Each mixture was stirred for 30 min followed by sonication for 15 min at room temperature. The mixed dispersion was then coated on a glass plates with similar surface areas (0.8 × 2.5 cm^2) and allowed to dry under the ambient conditions of the laboratory. After drying, samples were annealed at 100°C close to T_g of PMMA for 10 min to complete film formation process of PMMA particles. After annealing step, films were removed from the oven and cooled down to room temperature.

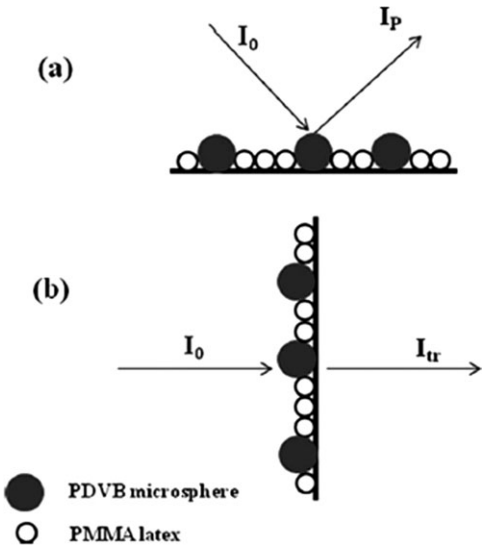


FIG. 2. Schematic illustration of sample position and (a) incident light (I_o), monomer (I_P) intensities and (b) transmitted light intensity (I_{tr}).

Measurements

In fluorescence measurements for oxygen diffusion experiments, films were placed in a round quartz tube filled with nitrogen, in Perkin Elmer Model LS-50 fluorescence spectrophotometer. Slit widths were kept at 8 nm. All measurements were carried out at room temperature of 24°C. In all experiments, *P* was excited at 345 nm and the intensity at the emission maximum (395 nm) was used for the *P* intensity (I_p) measurements. *P* intensity, I_p, was monitored against time for different PDVB content composite film after the quartz tube was open to the air for oxygen diffusion experiments by using time-drive mode of spectrophotometer. Because the diffusion measurements required that oxygen permeate only one surface of the film, a small region in the center of the films was masked off for measurement using black tape on the opposite side of the window from the samples. The sample position, incident light, I_o, and pyrene intensities I_P, are shown in Fig. 2a.

PT experiments were carried out using Variant Carry-100 UVV spectrometer. The transmittances of the films were detected at 500 nm. A glass plate was used as a standard for all UVV experiments and measurements were carried out at room temperature after each annealing process. The sample position and the transmitted light intensity, I_{tr}, are presented in Fig. 2b. Scanning electron microscope (SEM) images were taken by using LEO Supra VP35 FESEM.

Percolation

Initially, the percolation theory has been associated with a paper of Broadbent and Hammersley which

DOI 10.1002/pc

discussed the general situation of a fluid spreading randomly through a medium [31]. The most interesting feature of percolation phenomenon is the existence of a percolation threshold, p_c below which spreading process is confined to be a finite region. The spread of a blight from tree to tree in an orchard was discussed by Broadbent and Hammersley where the trees are planted on intersection of a square lattice. The percolation threshold, p_c for this problem is around 0.6 for so called "site percolation" on a square lattice. In other example is the seepage of water in the cracks and fractures of a rock formation. A similar problem for practical interest is the spread of water displacing oil in porous rocks, where neighboring pores are connected by small capillary channels [32]. If no oil in the system injected water into any given pore may only invade another pore through capillary channels or "bonds." The pores are "sites" connected to the chosen center of injection form what is called a "cluster." The largest cluster spans the lattice connecting the left and right edges to the bottom edge, which is called "percolating cluster." The percolation probability, $p_\infty(p)$, is defined as the probability that water injected at a site, chosen at random, will wet infinitely many pores. Here, one has to be noticed that the probability for having a pore at all the sites where water injection is attempted is p. Extensive simulations and theoretical work have shown that the percolation probability vanishes as a power-law near p_c.

$$p_\infty(p) \approx (p - p_c)^\beta \quad (\text{for } p > p_c, \text{ and } p \rightarrow p) \tag{1}$$

In a simple cubic lattice, p_c is found to be 0.31 for site-percolation and 0.25 for bond percolation models [33]. The exponent β for a simple cubic lattice is 0.42, for percolation model; however, β is very close to 1.0 in classical model [33].

Oxygen Diffusion

Stern-Volmer Kinetics. When samples containing fluorescent probes are exposed to air or their solutions saturated with oxygen, the fluorescence intensities of the samples decrease and the rates of fluorescence decay increase. These phenomena are due to oxygen quenching of the probe's excited state. The mechanism of quenching involves a sequence of spin allowed internal conversion processes which takes place within a weakly associated encounter complex between probe and oxygen. The product is either a singlet ground state or an excited triplet species [34].

Data generated from oxygen quenching studies on small molecules in homogeneous environment are usually analyzed using the Stern-Volmer relation given below, provided that the oxygen concentration $[O_2]$ is not too high [35]

$$\frac{I_0}{I} = 1 + k_q \tau_0 [O_2] \tag{2}$$

In this equation, I and I_o are the fluorescence intensities in the presence and absence of oxygen, respectively, k_q is the bimolecular quenching rate constant, and τ_0 is the fluorescence lifetime in the absence of O_2. This equation requires that the decay of fluorescence is single exponential and, moreover, that quenching interactions occur with a unique rate constant k_q. From the slope of a plot of I_o/I versus $[O_2]$, k_q can be determined provided that τ_o is known. Diffusion coefficients related to the quenching events can be calculated from the time-independent Smoluchowski-Einstein [35] equation,

$$k_q = \frac{4\pi N_A (D_P + D_q) pR}{1000} \tag{3}$$

where D_P and D_q are diffusion coefficients of the excited probe and quencher, respectively, p is the quenching probability per collision, R is the sum of the collision radii ($R_P + R_q$), and N_A is Avagadro's number. *Equations 2* and *3* can also be applied to the case of quenching of polymer-bound excited states in glass as long as the fluorescence decay is exponential and k_q is single valued. A simplifying factor in the interpretation of k_q is the general assumption that $D_P << D_q$ when the probe is covalently attached to a polymer. For quenchers as small as molecular oxygen, such an assumption would not be unwarranted. On the time scale of fluorescence, the overall translational diffusion coefficient of the polymer coil is usually not important; the relevant diffusion coefficient is that for motion of individual chain segments.

Fickian Diffusion

Fick's second law of diffusion was used to model diffusion phenomena in plane sheet. The following equation is obtained by assuming a constant diffusion coefficient, for concentration changes in time [36]

$$\frac{C}{C_0} = \frac{x}{d} + \frac{2}{\pi} \sum_{n=1}^{\infty} \frac{\cos\, n\pi}{n} \sin \frac{n\pi x}{d} \exp\left(-\frac{Dn^2\pi^2 t}{d^2}\right) \tag{4}$$

where d is the thickness of the slab, D is the diffusion coefficient of the diffusant, and C_o and C are the concentration of the diffusant at time zero and t, respectively. x corresponds to the distance at which C is measured. We can replace the concentration terms directly with the amount of diffusant, M by using the following relation:

$$M = \int_v C dV \tag{5}$$

when *Eq. 5* is considered for a volume element in the plane sheet and substituted in *Eq. 4*, the following solution is obtained [36]:

$$\frac{M_t}{M_\infty} = 1 - \frac{8}{\pi^2} \sum_{n=0}^{\infty} \frac{1}{(2n+1)^2} \exp\left(-\frac{D(2n+1)^2\pi^2 t}{d^2}\right) \tag{6}$$

where M_t and M represent the amounts of diffusant entering the plane sheet at time t and infinity, respectively.

RESULTS AND DISCUSSION

Photon Transmission

The change in transmittance of the composite films at 500 nm is shown in Fig. 3a for 0, 1.5, 3, 5, 10, 20, 40, and 60 wt% PDVB content. If the refractive indices of the two polymers are close, little scattering is expected. In general, light scattering is a function not only of the refractive index difference of the components but also of the size and shape of the dispersed-phase domains. Therefore, optical transmission measurements are a measure of the number and size of air voids in a polymer film [37]. Regardless of the void fraction, transmission decreases with increasing void radius. On the basis of the change of transmittance of the films, the structure evolution of the film could be described as follow: Despite the refractive indices of two polymers are somewhat different [38], the transparency of the film is related to the size of the particles and voids inside the film whichleads to light scattering. It has to be noted that I_{tr} decreases dramatically with increasing PDVB contents in the film. The low PDVB content blend films are optically more transparent than those with high PDVB content. The transparency of the latex film is mainly determined by the scattering of the light that is dependent on the size of different polymer phases and the voids in the film [37]. When the size of polymer phases and the voids are bigger than the wavelength of irradiation light, the light scatters, and as a result, the transparency decreases. The plots of the I_{tr} versus PDVB content in Fig. 3a also confirm this hypothesis. As the PDVB content increased, (I_{tr}) decreased, indicating that low transparency occurs at higher PDVB content. Scattering centers in the film are increased as PDVB content is increased. Thus, more light is scattered and, as a result, optical transmission of films is decreased. Because the size of PDVB particles is large with respect to the wavelength of the visible light, the light is scattered resulting in low transparency in the film [39]. This behavior of I_{tr} can be explained by percolating PDVB particles in PMMA lattice.

Critical Exponents

The above findings can be rationalized by first assuming that $P_\infty(p)$ is proportional to the transmitted light intensity, I_{tr}. Second assumption can be made by using the following ratio

$$R = \frac{M_{PDVB}}{M_{PDVB} + M_{PMMA}} \tag{7}$$

where M_{PDVB} and M_{PMMA} present the weight of PDVB and PMMA in the film. If R is assumed to be the occupation probability, p of PDVB in the PMMA lattice, then the percolation threshold, P_c becomes R_c, and *Eq. 1* can be written as

$$I_{tr}(R) = (R - R_c)^{\beta} \tag{8}$$

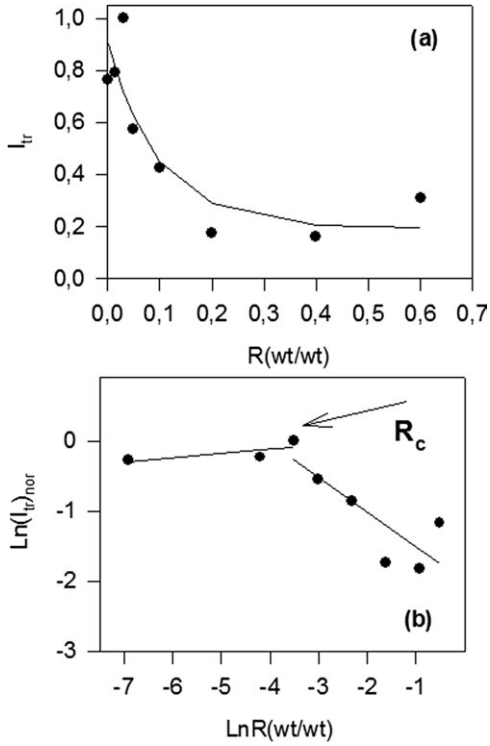


FIG. 3. (a) A plot of the transmitted photon intensities (I_{tr}) versus PDVB content, R (wt/wt) and (b) log–log plot of (I_{tr}) versus log R (wt/wt).

Equation 8 describes the percolation model for PDVB distribution in PMMA lattice. When R approaches R_c, the largest cluster of PDVB appears by connecting the left and right edges to the bottom edge of the PDVB. It is seen in Fig. 3a that inclusion of PDVB into PMMA lattice strongly decreases the transmitted light intensity.

On the other hand, the maxima of transmitted light intensity $1 - (I_{tr})$ versus PDVB content are also plotted in Fig. 4a, where it is seen that $1 \times (I_{tr})$ has increased to high values for all samples above 3 wt% PDVB content. This behavior of scanning light intensity can be explained by percolating PDVB particles in PMMA lattice. In Figs. 3b and 4b, log–log plot of *Eq. 4* is fitted to the data in Fig. 3a, where the slope of the straight line produced percolation threshold and the critical exponent, $R_c = 0.03$ and $\beta = 0.34$, which are not so far from site-percolation theory. In a simple cubic lattice, β is found to be 0.25 for site percolation model [31, 32]. In our previous study [40], to be able to see distribution of PNIPAM in PS lattice, we applied the percolation model and found $\beta = 0.91$. This value is very close to $\beta = 1.0$ as in classical model [31, 32].

To gain more insight into these phenomena, oxygen diffusion mechanism and their formulations were proposed.

Oxygen Diffusion

In Fig. 5, typical pyrene intensity, I_p, curves are presented against diffusion time for films having different PDVB content, exposed to oxygen. It is seen that as oxygen diffused through the film, the emission intensity of the pyrene decreased according to *Eq. 2*. The intensity

 DOI 10.1002/pc

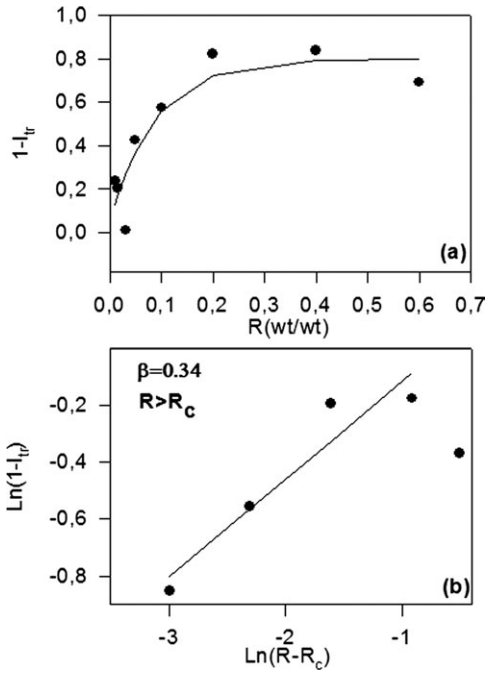


FIG. 4. Scattering light intensity, $1 - I_{tr}$, and its best fitted curve versus PDVB content: (a) R (wt/wt) and (b) log–log plot of the best fitted curve of $1 - I_{tr}$ versus $(R - R_c)$.

was saturated for all film samples once oxygen diffused through and equilibrated in the film. Here, it has to be noted that the quenching rate for high PDVB content film is higher than that for low PDVB content films predicting the more rapid quenching of excited pyrenes by O_2 molecules diffused into the high PDVB content composite films. All curves behave almost in the same fashion, as oxygen diffused through and equilibrated in the film. It is also seen that the diffusion curves reach their equilibrium value at shorter times for low PDVB content films. To interpret the above findings, *Eq. 2* can be expanded in a series for low quenching efficiency, i.e., $k_q\tau_0[O_2] << 1$ which then produces the following useful result

$$I \approx I_0\left(1 - k_q\tau_0[O_2]\right) \tag{9}$$

During O_2 diffusion into the latex films, P molecules are quenched in the volume which is occupied by O_2 molecules at time, t. Then, P intensity at time t can be represented by the volume integration of *Eq. 9* as

$$I_t = \frac{\int I dv}{\int dv} = I_0 - \frac{k_q\tau_0 I_0}{V}\int dv[O_2] \tag{10}$$

where dv and V are the differential and total volume of composite film, respectively, presented in Fig. 6. Performing the integration the following relation is obtained

$$I_t = I_0\left(1 - k_q\frac{\tau_0}{V}O_2(t)\right) \tag{11}$$

where $O_2(t) = \int dv\lfloor O_2 \rfloor$ is the amount of oxygen molecules diffuse into the latex film at time t.

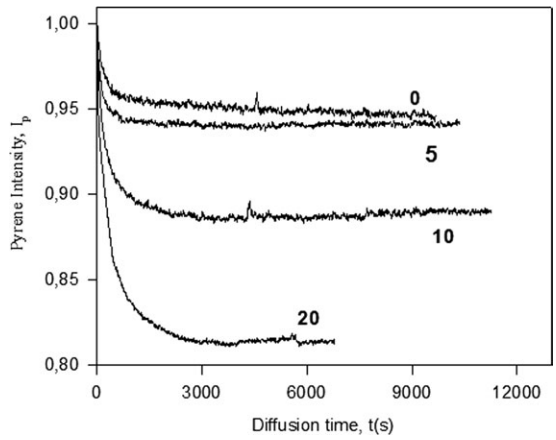


FIG. 5. The time behavior of pyrene, P, fluorescence intensity, I, during oxygen diffusion into the composite films with different PDVB content. Numbers on each curve indicates the PDVB content (%) in the film.

Combining *Eq. 9* with the Fick's law (*Eq. 5*), the fluorescence intensity change due to change in oxygen concentration is related to the time. If it is assumed that $O_2(t)$ corresponds to M_t, then *Eq. 11* can be combined for oxygen with *Eq. 6*. Combining *Eq. 6* for $n = 0$ for oxygen diffusion with *Eq. 11*, the following useful relation is obtained to interpret the diffusion curves in Fig. 5

$$\frac{I_t}{I_0} = A + \frac{8C}{\pi^2}\exp\left(-\frac{D\pi^2 t}{d^2}\right) \tag{12}$$

where $C = \frac{k_q\tau_0 O_2(\infty)}{V}$ and A=1−C . Here, $O_2(\infty)$ is the amount of oxygen molecules diffuse into latex film at time infinity. The logarithmic form of *Eq. 12* can be written as follows:

$$\mathrm{Ln}\left(\frac{I_t}{I_0} - A\right) = \mathrm{Ln}\left(\frac{8C}{\pi^2}\right) - \frac{D\pi^2}{d^2}t \tag{13}$$

This model is fitted with the experimental data using a linear least-squares fitting method to extract both k_q and diffusion coefficient (D) values. Figure 7 shows logarithmic plot ($\mathrm{Ln}(I_t/I_0 - A)$) of the data in Fig. 5 versus diffusion time for various PDVB content films. The solid lines represent the best fit to the diffusion model (*Eq. 13*).

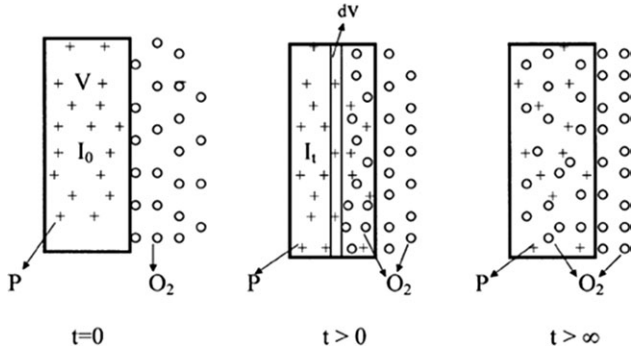


FIG. 6. Cartoon representation of oxygen diffusion into a latex film.

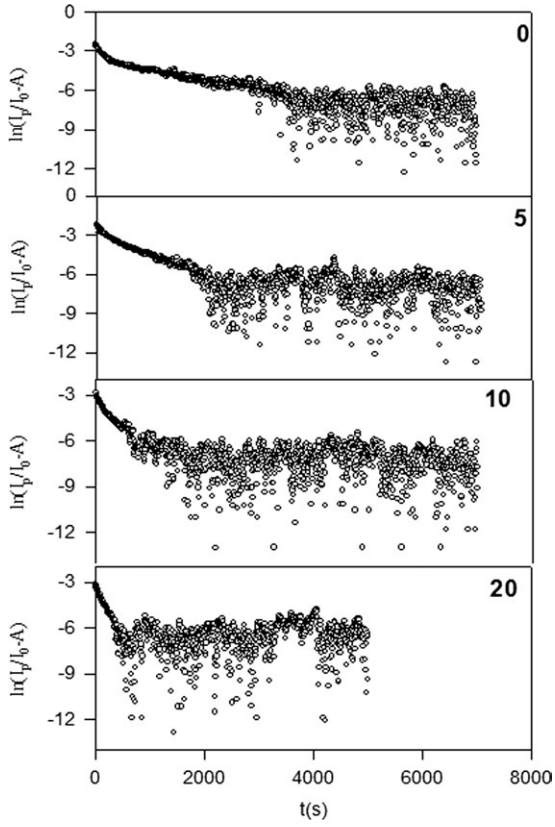


FIG. 7. Logarithmic plots of data in Fig. 5 and their fits to *Eq. 13* for (a) 0, (b) 5, (c) 10, and (d) 20 wt% PDVB content films.

Thus, we can extract information about both k_q and D by fitting *Eq. 10* to the data in Fig. 5. Here, k_q values were calculated from C. The produced k_q and D values are listed in Table 1. The reproducibility of the results was evaluated by performing five measurements per sample. As seen from the Table 1, diffusion coefficients of oxygen, D, are found to be strongly dependent on PDVB fraction in the film. The plot of D values versus W_{PDVB} (wt%) is shown in Fig. 8. Diffusion coefficients increase as the weight percentage of PDVB latex increases in PMMA. R_c = 0.03 value which founded from the percolation is very close to 0.05 (PDVB 5 wt%). Oxygen diffusion starts to accelerate with this PDVB content. As a result of adding PDVB, more voids become between the particles in the film and light scatters from these voids and the passing lihgt intensity decreases. These findings are consisting with oxygen diffusion process.

TABLE 1. Experimentally obtained diffusion (D) and mutual diffusion (D_m) coefficients.

PDVB (wt%)	D (cm^2 s^{-1}) × 10^{-11}	D_m (cm^2 s^{-1}) × 10^{-5}
0	1.8 ± 0.002	0.025 ± 0.002
5	2.8 ± 0.1	0.039 ± 0.007
10	10.8 ± 0.3	0.028 ± 0.002
20	36.6 ± 3.2	0.023 ± 0.003

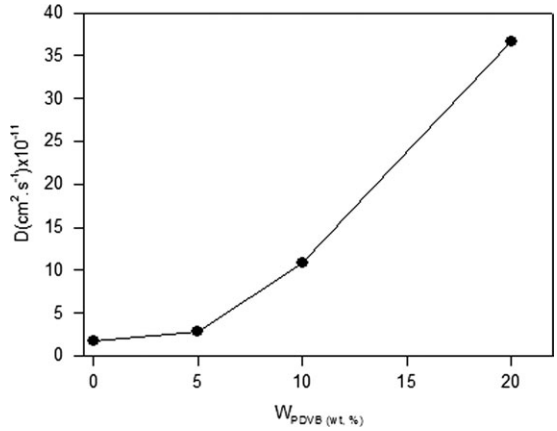


FIG. 8. Plot of the diffusion coefficient, D versus W_{PDVB} (wt%).

PDVB particles size are about five times bigger than PMMA particles. Voids between the PDVB and PMMA latex appeared allowing oxygen molecules to move rapidly. Therefore, O_2 molecules can easily pass through these voids. Thus, the permeability of O_2 gas is increased, yielding high diffusion coefficients. As a result, more rapid diffusion of oxygen [34] into composite films occurs due to the presence of a large number of microvoids in these films.

To support these findings, SEM was used to examine the morphologies of PMMA/PDVB composite films. Figure 9 presents SEM photographs of the films which have 0, 5, 20, and 40 wt% PDVB content annealed at 100°C. The SEM images of the films annealed at 100°C show that the surface of the composite films is very rough. These results reveal that 100°C, close to the T_g of PMMA, is too low to make the particles deform and retain their spherical shapes. Most of the light scatters due to the rough surface of the films which results low transmitted light intensity. Here, the small particles are PMMA latexes, whereas the large ones are crosslinked PDVB microspheres.

From SEM photographs of pure PMMA film (Fig. 9a), it can be seen that there is a low proportion of pores present. However, addition of 5, 20, and 40 wt% PDVB into the composite film (Fig. 9b–d) creates higher voids structure in the film. These structure accelerates the diffusion rate of oxygen along the film by decreasing the surface area for diffusing oxygen molecules in consistent with the increase in D values.

On the other hand, D values for this study (10^{-11} cm^2 s^{-1}) is found to be one order smaller than that of PS/PNIPAM films (10^{-10} cm^2 s^{-1}) annealed at various temperatures [41]. This difference shows that the rate of oxygen diffusion in PS/PNIPAM composite films through the voids is much faster than the diffusion rate of oxygen through PMMA/PDVB polymer matrix. This difference can be originated from the absence of voids in PMMA/PDVB films due to the formation of a mechanically strong, void-free continuous matrix which hinders the diffusive processes from the film surface.

DOI 10.1002/pc

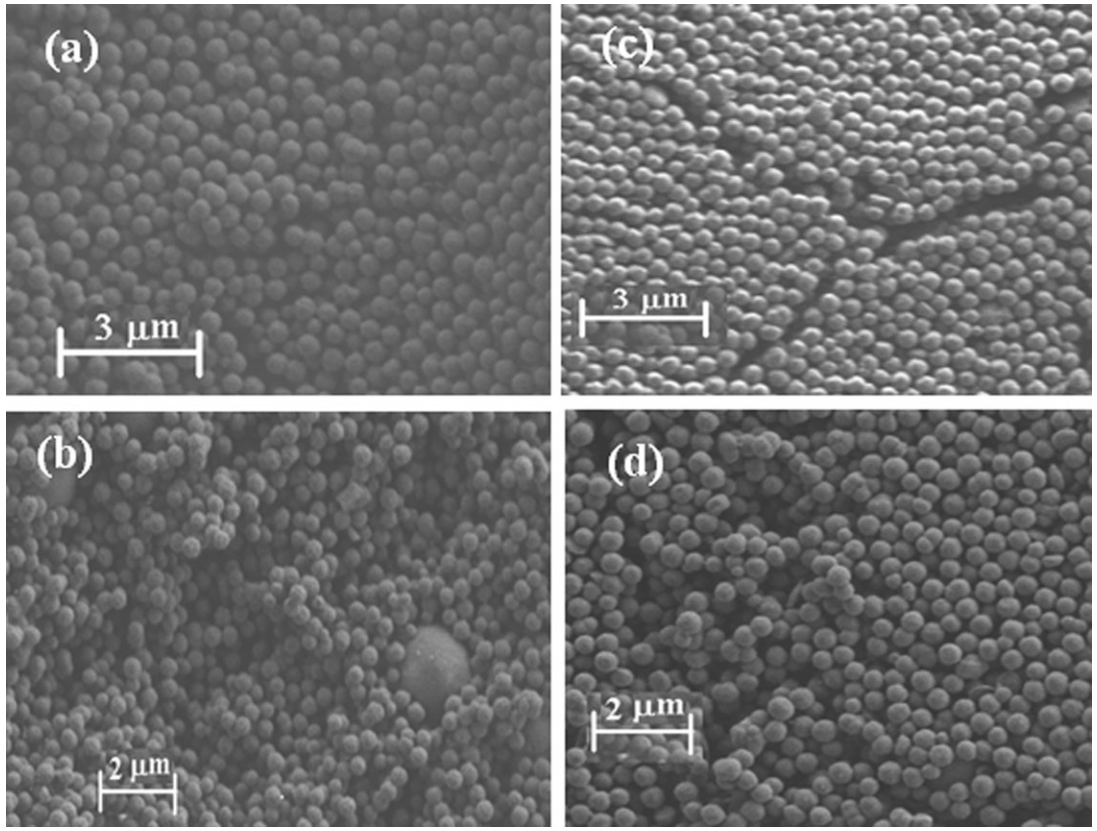


FIG. 9. SEM images of composite films prepared with 0, 5, 20, and 40% PDVB content and annealed for 10 min at 100°C temperature.

When the pyrene diffusion in the latex film is omitted and $p = 1$ is taken then *Eq. 3* becomes as

$$k_q = \frac{4\pi N_A D_m R}{1000} \tag{14}$$

Here, D_m is called as mutual diffusion coefficient which can now be assumed to be the self diffusion coefficient of O_2 in the composite film. Because k_q is known and if R is taken as the radius of pyrene [42], then the averaged D_m values were obtained and listed in Table 1 for the composite films having different PDVB content.

It is seen in Table 1 that D_m is independent of PDVB content in composite films, i.e., once O_2 penetrates into the film then it moves in short range independent of the material structure. D_m value obtained in the present study (10^{-5} cm^2 s^{-1}) is one order larger than that previously obtained (10^{-6} cm^2 s^{-1}) by using the same technique [42]. This shows that the voids in composite films reduce of pyrene and O_2 molecules response time.

CONCLUSIONS

This work has shown that it is possible to measure the diffusion coefficient of oxygen molecules penetrating into composite films quite accurately by using simple SSF technique.

Diffusion experiments demonstrated that the quenching rate during oxygen diffusion was completely consistent with Fickian diffusion. It was understood that the addition of PDVB into PMMA matrix creates more voids in the film which results faster diffusion of oxygen into the composite film. The results showed that PDVB content has presented serious effects on the properties of the composite matrix formed from PMMA particles. Optical transparency percolation was found around 3 wt% PDVB content. On the other hand, results suggest that self-diffusion of oxygen molecules in the composite films are not affected by the size and the structure of the composite films. In other words, D_m values give information only on local environment.

REFERENCES

1. T.-W. Chou, "Structure and Properties of Composites," in *Materials Science and Technology,* **13**, R.W. Cahn, P. Haasen, and E.J. Kramer, Eds., VCH Weinheim (1993).
2. R.A. Vara, K.D. Jandt, F.J. Kramer, and F.P. Giannelis, *Chem. Mater*., **8**, 2628 (1996).
3. M.W. Noh and D.C. Lee, *Polym. Bull*., **42**, 619 (1999).
4. H.Z. Friedlander, and C.R. Grink, *J. Polym. Sci. Part B: Polym. Lett*., **2**, 475 (1964).
5. C. Kato, K. Kuroda, and H. Takahara, *Clay Clay Miner.*, **29**, 294 (1981).

6. J.G. Doh and I. Cho, *Polym. Bull*., **41**, 511 (1998).
7. Z. Ji, R.E. Majors, and E.J. Guthrie, *J. Chromatogr. A*, **842**, 115 (1999).
8. J.Y. Li, S. Ichizuri, S. Asano, F. Mutou, S. Ikeda, M. Lida, T. Miura, A. Oshima, Y. Tabata and M. Washio. *J. Appl. Polym. Sci*., **101**, 3587 (2006).
9. S. Savari, S. Sachdeva, and A. Kumar, *J. Membr. Sci*., **310**, 246 (2008).
10. M. Matsuguchi, Y. Kadowaki, K. Noda, and R. Naganawa. *Sens. Actuators B*, **120**, 462 (2007).
11. R. Molina, A. Vilchez, C. Canal, and Esquena J. *Surf. Interface Anal*., **41**, 371 (2009).
12. G. Shaw, *Trans. Faraday Soc*., **63**, 2181 (1967).
13. R.E. Barker, *J. Polym. Sci*., **58**, 553 (1962).
14. J.R. Mac Callum, and A.L. Rudkin, *Eur. Polym. J*., **14**, 655 (1978).
15. M.E. Cox, *J. Polym. Sci*., **24**, 621 (1986).
16. M.E. Cox, and B. Dunn, *J. Polym. Sci*., **24**, 2395 (1986).
17. J.R. MacCallum, and A.L. Ruddin, *Eur. Polym. J*., **14**, 655 (1978).
18. X. Lu, I. Manners, and M.A. Winnik, in Oxygen Diffusion in Polymer Films For Luminescence Barometry Applications, *Fluorescence Spectroscopy; New Trends in Fluorescence Spectroscopy*, B. Valuer and J.C. Brochan, Eds., Springer Verlag, New York, Chapter **12**, 229 (2001).
19. C.N. Jayarajah, A. Yekta, I. Manners, and M.A. Winnik, *Macromolecules*, **33**, 5693 (2000).
20. R. Ruffolo, C. Evans, X.H. Liu, Y. Ni, Z. Pang, P. Park, A. MacWilliams, X. Gu, X. Lu, A. Yekta, M.A. Winnik, and I. Manners, *Anal. Chem*., **72**, 1894 (2000).
21. O. Pekcan, and S. Ugur, *J. Colloid Interface Sci*., **217**, 154 (1999).
22. O. Pekcan, and S. Ugur, *Polymer*, **41**, 7531 (2000).
23. O. Pekcan, M.A. Winnik, and L. Egan, *Macromolecules*, **16**, 702 (1983).
24. M.A. Winnik, O. Pekcan, and L. Egan, *Polymer*, **25**, 1767 (1984).
25. M.A. Winnik, O. Pekcan, and L. Chen, *Macromolecules*, **21**, 55 (1988).
26. B. Karagoz, Y.Y. Durmaz, B.N. Gacal, N. Bicak, and Y. Yagci, *Des. Mon. Polym*., **12**, 511 (2009).
27. K. Li and H.D.H. Stover, *J. Polym. Sci. Part A: Polym. Chem*., **31**, 3257 (1993).
28. F. Lime and K. Irgum, *J. Polym. Sci. Part A: Polym. Chem*., **47**, 1259 (2009).
29. A. Nyhus, S. Hagen, and A. Berge, *J. Polym. Sci. Part A: Polym. Chem*., **38**, 1366 (2000).
30. B.N. Gacal, B. Koz, B. Gacal, B. Kiskan, M. Erdogan, and Y. Yagci, *J. Polym. Sci. Part A: Polym. Chem*., **47**, 1317 (2009).
31. S.R. Broadbent and J.M. Hammersley, *Proc. Cambridge Philos. Soc*. **53**, 629 (1957).
32. M. Sahimi, *Applications of Percolation Theory*, *Taylor and Francis, London*, 1994.
33. D. Stauffer, *Introduction to Percolation Theory*, *Taylor and Francis, London*, 1985.
34. J.B. Birks, *Organic Molecular Photophysics*, *Wiley-Interscience, New York*, 1975.
35. S.A. Rice, "Diffusion-Limited Reactions," in *Comprehensive Chemical Kinetics*, C.H. Bamford, C.F.H. Tipper, and R.G. Compton, Eds., Elsevier, Amsterdam, 25, 1985.
36. J. Crank, *The Mathematics of Diffusion*, *Oxford University Press, London*, 1970.
37. G.H. Meeten, *Optical Properties of Polymers*, Elsevier Applied Science Publishers, London, 29 (1986).
38. L. Bohn, in *Polymer Handbook*, 2nd ed., J. Brandup and E.H. Immergut, Eds., Wiley-Interscience, New York, 1975.
39. J.L. Keddie, P. Meredith, R.A.L. Jones, and A.M. Donald, *Langmuir*, **12**, 3793 (1996).
40. S. Ugur, O. Yargi, and O. Pekcan, *Polym. Compos*., **2**, 179, (2008).
41. O. Pekcan and S. Ugur, *J. Colloid Interface Sci*., **217**, 154, (1999).
42. O. Pekcan and S. Ugur, *Polymer*, **41**, 7531, (2000).

 DOI 10.1002/pc